Scalable Computing: Practice and Experience, ISSN 1895-1767, http://www.scpe.org
© 2024 SCPE. Volume 25, Issues 6, pp. 5227–5239, DOI 10.12694/scpe.v25i6.3318

UPPER LIMB REHABILITATION ROBOTS TRAINING ANALYSIS BASED ON MULTI-SENSOR TRAJECTORY DATA AND HUMAN-COMPUTER INTERACTION

YANYU LIU* AND XIANQIAN LAO†

Abstract. Upper limb rehabilitation robots have important practical significance in helping patients recover their motor function, but traditional training methods often lack real-time and accurate evaluation of patient movement status and intention and have low interactive participation. Therefore, the study proposes a training system for upper limb rehabilitation robots based on multi-sensor trajectory data and human-computer interaction. The system is designed from three aspects: inertial sensor trajectory tracking, Kinect sensor image restoration, and interaction system design. A polynomial joint zero value constraint algorithm is introduced to correct errors, and variable parameter pixel filtering combined with a weighted average moving algorithm is used to improve image quality. The training results showed that the robot trajectory tracking accuracy significantly improved, and the improvement in motion trajectory error was greater than 20%. Compared with traditional training methods, interactive training had a recognition accuracy of over 85% in rehabilitation actions, and the system had better stability. This rehabilitation robot can effectively meet the feasibility and effectiveness of improving the interaction system, providing new technological means for intelligent medical services.

Key words: Inertial sensor; Trajectory data; Human computer interaction; Rehabilitation robots; Sports intention

1. Introduction. With the acceleration of social aging and the frequent occurrence of work-related accidents, the rehabilitation of upper limb motor dysfunction has received widespread attention from society. Among them, upper limb rehabilitation robots, as a new type of rehabilitation treatment method, aim to help patients recover their upper limb motor function through mechanical-assisted training. Moreover, early rehabilitation robots are mostly end traction type with a simple structure, resulting in lower control requirements and equipment costs. However, their guidance of joint strength is not precise enough, and their degree of freedom of movement and traction treatment safety are also low [1-2]. With the continuous development of control theory and artificial intelligence technology, rehabilitation therapy robots are also constantly improving in joint support, motion degrees of freedom, and other aspects based on the laws of human spontaneous movement. The acceleration of social aging and frequent accidents have led to an increasing demand for rehabilitation treatment. However, traditional rehabilitation methods have limited resources and are difficult to meet rehabilitation needs. Early rehabilitation robots have shortcomings in joint strength guidance, freedom of movement, and safety. Although traditional rehabilitation robot technology has made progress to some extent, they can accurately evaluate patient status in real-time There are still many challenges in adapting to personalized rehabilitation needs and improving patient engagement. Most existing rehabilitation robots often use a single sensor system, which limits their ability to capture complex upper limb activity dynamics, resulting in insufficient motion guidance and feedback. Therefore, to further promote the development of rehabilitation robot training technology, meet the growing rehabilitation needs, and promote the development of rehabilitation medical science, a training system based on sensor data and human-computer interaction is proposed. By capturing the patient's movement status and intention and applying interaction methods, the rehabilitation effect is improved.

Xiao W et al. developed a bilateral upper limb collaborative rehabilitation robot system based on mirror therapy and virtual stimulation. The affected limb can track healthy limbs for radial movement with the assistance of a robotic arm, and rehabilitation training based on neural networks and controllers can provide good visual stimulation. The results indicated that the system effectively completed rehabilitation training and improved patients' awareness of active rehabilitation [3]. Y Wang et al. achieved clinical rehabilitation

*School of Electronic Information Engineering, Beihai Vocational College, Beihai, 536000, China (liuyanyu@bhzyxy.edu.cn)
†School of Electronic Information Engineering, Beihai Vocational College, Beihai, 536000, China (xianqianlao2023@163.com)

equipment design by segmenting and classifying the surface electromyographic signals of patients and processing them through signal encoding processing, transformation, and waveform classification comparison. The results showed that the signal classification had high accuracy [4]. Q Sun et al. believe that human-computer interaction can be achieved through rehabilitation training trajectories and simulation design can be carried out through the establishment of motion constraint equations and the acquisition of collaborative space. The results indicated that the designed indicators provided a good reference for the selection of training trajectories for rehabilitation robots [5]. Yousuf F H et al. designed an upper limb amputee rehabilitation system using SEMG sensors and stimulated hand movement using a robot simulator toolkit. The results indicated that the design approach had good effectiveness, but the sample size selected for testing was relatively small [6]. Chen X et al. developed a new type of soft and wearable upper limb rehabilitation robot, which can perform rehabilitation training for wrist and elbow joints. The results of wrist rehabilitation training indicated that this design approach effectively improved the flexibility, comfort, and safety of training [7]. Wu Q et al. proposed an adaptive neural collaborative control strategy to achieve intention-based human-machine collaborative rehabilitation training, and obtained muscle force data using surface electromyography signals and Kalman filtering. The results showed that this control strategy had good cooperation [8].

Whether it is using neural networks to design rehabilitation training systems, analyzing electromyographic signals, or introducing human-computer interaction to train robot trajectories, the essence lies in extracting information data related to patient movement. Therefore, the study utilizes multi-sensor trajectory data to achieve real-time and accurate acquisition of patient movement status and intention, and introduces the advantages of human-computer interaction into the design of training systems, to provide a more natural and comfortable user experience and improve the rehabilitation training effect of patients. Multi-sensor trajectory data can obtain real-time and accurate patient movement status and intention, while human-computer interaction technology can provide patients with a more natural and comfortable user experience during the use of robots, improving the rehabilitation training effect of patients. The research mainly demonstrates four aspects. The first part is a literature review of the current application technology of rehabilitation robots. The second part is the method design of inertial sensors, Kinect sensors, and human-computer interaction. The third part is the result verification of the training method proposed in the study. The last part is a summary of the entire article.

2. Related works. To meet the rehabilitation needs of stroke patients due to different disabilities, scholar X Li proposed an upper limb rehabilitation robot that can be used under hybrid control driven by flexible cables and designed different working modes to provide assistance to the subjects. The experimental results showed that this method adaptively adjusted the damping force and stiffness coefficient, adjusted the working mode according to the motion performance of the subjects, and had good application performance [9]. Q Meng et al. designed a lightweight upper limb rehabilitation robot with a spatial training function using a 4-degree-of-freedom end effector. The experimental results showed that the component had high flexibility (over 60%) and a large workspace, and passed joint training and drinking water trajectory planning experiments [10]. In response to the low participation problem of on-demand auxiliary controllers in robot-assisted rehabilitation, J Zhang et al. designed an adaptive controller by adjusting the trial-and-error participation estimation and energy information evaluation. The results indicated that this method effectively reduced the energy consumption of subjects (more than 30%), helping them improve the effectiveness of upper limb rehabilitation [11]. In response to the problem of parameter uncertainty in the dynamic modeling of upper limb rehabilitation robots, JL Wang et al. used a variable parameter particle swarm optimization algorithm for identification improvement. Simulation results showed that the algorithm improved identification accuracy and control effectiveness [12]. To solve the control problem of upper limb rehabilitation robots, N Mirrashid et al. proposed a fuzzy controller based on an ant colony optimization algorithm to achieve controller gain adjustment. The results indicated that the tracking error of the improved algorithm was much smaller than the original results [13]. To improve the effectiveness of rehabilitation treatment, scholar Q Wu proposed a control strategy combining adaptive neural collaboration and Gaussian radial basis function network to obtain human motion intention and muscle force data. The experimental results showed that this strategy had the potential to regulate interaction compliance and collaboration, demonstrating good accuracy and stability [14].

Traditional upper limb rehabilitation robots are unable to control patients based on their movement inten-

tions, resulting in low patient engagement. Therefore, scholar Q Meng proposed an upper limb rehabilitation robot based on electromyographic signal motion compensation control. The experiment verified that the control method demonstrated good performance in electromyographic compensation and trajectory execution [15]. C Rossa scholars proposed a robot-assisted model based on the eight degrees of freedom kinematics of the upper limbs to address the current situation of disability abilities. The results showed that the auxiliary robot effectively achieved spatial motion range matching, and the framework system was suitable for patient rehabilitation treatment [16]. J Zhou et al. proposed to improve the trajectory tracking performance of lower limb rehabilitation robots using a trajectory deformation algorithm and low-order proportional differentiation. The results showed that the robots designed by this method had good application potential in the field of assisted rehabilitation [17]. Scholar Li proposed a rehabilitation robot action recognition method based on multi-channel surface electromyography signals, which extracted motion features through bilateral mirror training and electromyography signal constraint processing. The results indicated that this method had faster convergence speed and better extraction accuracy [18]. S Cai scholars analyzed the feasibility of compensation for stroke patients based on pressure distribution data and support vector machine algorithm, and the results showed that this method had good classification performance in compensation analysis [19]. T Proietti proposed a multi-joint soft wearable robot based on textiles to assist upper limb rehabilitation training. The results showed that the robot achieved dynamic gravity compensation and joint trajectory tracking and demonstrated good performance and application potential in rehabilitation training [20].

Sensors can be combined with human motion to obtain motion information and estimate and track the wearer's posture and motion trajectory. Obtaining motion data information through sensors has become an important aspect of scientific research. Among them, Assad Uz Zaman M utilized Kinect V2 sensors to achieve motion tracking of robots, and based on sensor data, developed a solution that solved the inverse kinematics of upper limbs, which provided application ideas for remote rehabilitation treatment [21]. Azlan N Z et al. utilized an on-demand auxiliary control strategy to adjust sensor information in robot-assisted rehabilitation therapy. The results showed that the proposed control strategy effectively drove the upper limb rehabilitation robot to achieve zero steady-state error [22]. Tongtong Z et al. proposed a novel 7-degree-of-freedom upper limb exoskeleton robot, which replaced the grip of traditional exoskeletons with a new hand fixation device. The rationality of robot drive selection was verified through the model of this scheme [23]. Regarding the issue of poor compatibility of upper limb rehabilitation robots, Yan H et al. established an equivalent mechanical model of the human upper limb based on its anatomical structure. The configuration synthesis of upper limb rehabilitation institutions was carried out. The results indicated that the 5Ra1P configuration of the shoulder joint had better kinematic performance [24].

In summary, for rehabilitation robots, most scholars mainly focus on optimizing and improving their adaptability and patient engagement, including adaptive controller design, hybrid control, and other aspects. Methods such as motion compensation, degree of freedom kinematic models, and support vector machines have also been applied in research on motion intention control. Upper limb rehabilitation robots and their treatment methods are gradually developing towards human-machine interaction training. More and more scholars and teachers are researching various human-machine interaction methods such as patient motion intention detection and estimation, motion information capture, virtual reality, etc. This not only increases the fun of rehabilitation treatment but also improves rehabilitation motion intention. Whether it is the introduction of adaptive controller design, hybrid control, motion compensation, degrees of freedom kinematic models, etc., how to efficiently and accurately obtain patient motion intentions, limb end motion trajectories, and other information is gradually becoming a research focus. Previous studies have combined sensors with human motion, often based on motion data or trajectory tracking results for capture and analysis. However, they have overlooked the susceptibility of sensors to external acceleration, magnetic interference, and cumulative errors during use, making it difficult for a single sensor to achieve good motion trajectory data acquisition. Based on the advantages of sensors, this study proposes an improved rehabilitation training system based on multi-sensor and human-computer interaction, aiming to meet the upper limb movement needs of patients and provide technical means for rehabilitation medicine.

3. Design of robot training method based on multi-sensor trajectory data and human-computer interaction. Accelerating the exploration of human-machine rehabilitation interactive training methods can

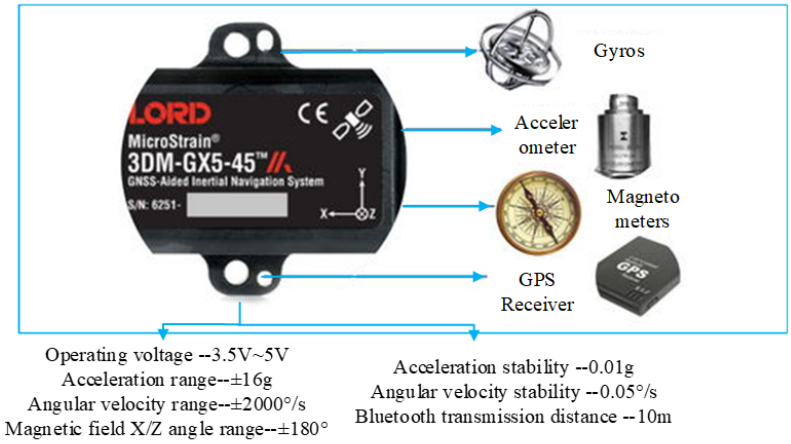

Fig. 3.1: Performance parameters of the selected inertial sensor

improve patient motivation and participation. Therefore, in the design of rehabilitation robot training, it is necessary to accurately capture the patient's movement intention and trajectory information. Therefore, research is conducted on designing trajectory-tracking algorithms based on inertial sensors and Kinect sensors, and improvements are made in data fusion processing, tracking error correction, motion data acquisition, and other aspects. The joint design of multiple sensors and human-computer interaction can better improve the quality of rehabilitation training for patients.

3.1. Design of trajectory tracking algorithm based on inertial sensors. Considering the need to fix the sensor on the patient during rehabilitation exercise therapy, the study was conducted by selecting a nine-axis wireless inertial sensor, which can be used as a sensor for monitoring tilt, vibration, rotation, and multi-degree-of-freedom motion, and it can ensure a long time of stable operation and light weight. Figure 3.1 shows the performance parameters of the inertial sensor.

The sensor is equipped with its communication protocol, and motion data can be transmitted through Bluetooth through the sensor. The Bluetooth receiver can be connected to the upper computer system through a USB port. Inertial sensors often use their coordinate system to determine reference data in three-dimensional space, and the geographic coordinate system of the motion information of these objects is different. Therefore, coordinate conversion is necessary first. The coordinate transformation can be explained using equation (3.1).

$$\begin{bmatrix} Xb \\ Yb \\ Zb \end{bmatrix} = C \begin{bmatrix} Xe \\ Ye \\ Ze \end{bmatrix} \tag{3.1}$$

In equation (3.1), $[Xe \quad Ye \quad Ze]$ represents the geographic coordinate system, $[Xb \quad Yb \quad Zb]$ represents the sensor coordinate system, and C represents the rotation orthogonal matrix. When inertial sensors perform attitude calculation, they mainly include three parts: data processing, attitude calculation, and updating. However, due to the influence of component performance and usage environment, there is inevitably a noise problem when the sensor collects data. Therefore, research is conducted to calibrate the sensor error and obtain the output model, as shown in equation (3.2).

$$ai(t) = \hat{a}i(t) + gi(t) + ba, i(t) + \varepsilon a, i(t) \tag{3.2}$$

In equation (3.2), t is the moment, i is the axis direction, $ai(t)$ is the output value of the accelerometer, $\hat{a}i(t)$ is the acceleration component, $gi(t)$ is the gravitational acceleration component, $ba, i(t)$ is the zero bias error of the accelerometer device, and $\varepsilon a, i(t)$ is Gaussian white noise. By performing acceleration zero correction

on sensors placed in a horizontal plane, their zero bias error can be corrected. The output model of gyroscope $wi(t)$ and magnetometer h is equation (3.3).

$$\begin{cases} wi(t) = \hat{w}i(t) + ba, i'(t) + \varepsilon a, i'(t) \\ h = AH + B + \varepsilon \end{cases} \tag{3.3}$$

In equation (3.3), $\hat{w}i(t), ba, i'(t), \varepsilon a, i'(t)$ represent the angular velocity, bias error, and Gaussian white noise of the gyroscope motion. A, B are the soft and hard magnetic interferences of the magnetometer, ε is the Gaussian white noise of the magnetometer, and H is the height. To improve the accuracy of attitude calculation and reduce errors, research is conducted on the estimation error correction and compensation of accelerometers, gyroscopes, and magnetometers after the fusion processing of three types of information using a gradient descent method. Equation (3.4) is the error function of accelerometer and magnetometer information.

$$f = \begin{bmatrix} e(gs, as) \\ e(hs, ms) \end{bmatrix} \tag{3.4}$$

In equation (3.4), hs is the magnetic field strength, gs is the quaternion of gravitational acceleration, as is the quaternion of the accelerometer, and ms is the quaternion of the magnetometer. Equation (3.5) is the quaternion attitude update for the fusion information error function.

$$qt + 1 = qt + 0.5qtwt\Delta t - \beta \frac{\nabla f}{\|\nabla f\|}\Delta t \tag{3.5}$$

In equation (3.5), β is the weight of the correction function, wt is the angular velocity matrix, and $qt+1, qt$ is the quaternion of the attitude at the next and current moments. Subsequently, the motion trajectory of the sensor acceleration signal is extracted, and the gravity acceleration component is removed during the extraction process to obtain the true acceleration information. The tracking algorithm is designed based on frequency domain numerical integration. It should also be noted that since trajectory data is obtained through integration processing, cumulative errors such as sensor errors and random errors can also affect the trajectory data results, causing them to deviate from the true trajectory and, in severe cases, leading to trajectory distortion [25]. Therefore, the study proposes cumulative error correction based on polynomials. Considering the insufficient number of motion constraints, a first-order polynomial is used for fitting to obtain the displacement correction, as shown in equation (3.6).

$$xc(t) = xc(t) + \frac{1}{2T}[v(0) - v(T)]t^2 - v(0)t - x(0) \tag{3.6}$$

In equation (3.6), $xc(t)$ represents the corrected displacement, $xc(t)$ represents the uncorrected velocity after integration, $v(0)$ is the initial velocity, $v(T)$ is the final velocity, and $x(0)$ is the initial displacement. As time goes on. Relying solely on polynomial correction for error control makes it difficult to effectively solve the problem of integration error after data collection. Therefore, considering the intermittent characteristics of human upper limbs during movement, this study introduces zero-value constraints into polynomial error correction methods. By setting an acceleration data threshold to manually correct the theoretically zero data during the tracking process, the displacement value in the stationary state can be obtained, as shown in equation (3.7).

$$xcorrrcted = \begin{cases} xc(t-1), vc < v\lim it \cap ac < a\lim it \\ xc(t), vc \geq v\lim it \cup ac \geq a\lim it \end{cases} \tag{3.7}$$

In equation (3.7), $v\lim it$ is the velocity threshold, $a\lim it$ is the displacement threshold, and a is the acceleration.

3.2. Human upper limb motion trajectory tracking based on Kinect sensors. . The upper limb rehabilitation training techniques are mainly improved through hip joint rotation, elbow joint flexion and extension, and other methods. With the continuous development of modern medical technology, rehabilitation

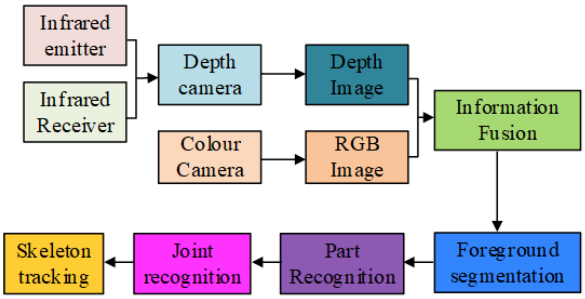

Fig. 3.2: Schematic diagram of Kinect sensor target tracking process

training systems based on intelligent sensors are receiving more and more attention [26]. Kinect sensor is a device based on visual and motion recognition technology launched by Microsoft, which can track the movement trajectory and posture of the human body in real-time, and collect depth data, bone data, and color data of the human body, with higher transmission rates [27]. In human upper limb rehabilitation exercise training, Kinect sensors can utilize their posture recognition function to assist rehabilitation patients in accurate and real-time motion monitoring and guidance and perform coordinate positioning and image processing based on the obtained data. Figure 3.2 shows the target tracking process of the sensor.

In Figure 3.2, the Kinect sensor utilizes depth images to track the skeleton framework. The grayscale values of each pixel in the image are the distance between a point in space and the camera. When the sensor tracks the target, it processes the obtained depth image information, performs foreground segmentation, identifies parts and joints, and constructs a three-dimensional coordinate system for the relevant nodes. Considering the possible deformation and distortion issues of the sensor camera lens during imaging, it is necessary to calibrate the camera. Research on reducing imaging interference during camera calibration by designing radial distortion coefficients. The distortion coefficient can be expressed as equation (3.8).

$$\begin{cases} Xa = Xb(1 + k1r^2 + k2r^4) \\ Ya = Yb(1 + k1r^2 + k2r^4) \end{cases} \tag{3.8}$$

In equation (3.8), Xb, Yb represent the coordinates before correction, Xa, Ya are the coordinates after correction, and $k1, k2$ are the distortion coefficients. The imaging information quality of Kinect sensors is closely related to the tracking function of the human skeletal framework, among which sensor performance limitations, surface material impact on reflectivity, environmental occlusion, etc. can all cause loss of depth image information. To reduce the loss of depth information caused by objective conditions, research proposes to repair depth images. Traditional filtering and denoising algorithms for images cannot effectively reduce the information loss areas in Kinect depth images, and to some extent, it will lead to changes in the depth values of the imaging areas. Therefore, the study proposes a repair algorithm based on variable parameter pixel filters to enhance the loss area. Figure 3.3 is a schematic diagram of the filter principle.

Pixel filters redefine the filtering area with candidate pixels as the center, set action thresholds for inner and outer filters, and compare and assign values to the number of pixels with the threshold. Due to the limited mobility of the target patients that the rehabilitation robot is facing, it mainly requires certain rehabilitation treatment in the upper limbs. Therefore, the study limited patients to engaging in activities within the range of Kinect sensor cameras. To achieve a balance between the image restoration effect and computational time, a certain area range was set for filter processing settings. The calculation equation for filter size and threshold is shown in equation (3.9).

$$\begin{aligned} Nineer &= \begin{cases} c1, u \in Z \cap v \in Z \\ c2, u \notin Z \cup v \notin Z \end{cases} \qquad Nouter = \begin{cases} c3, u \in Z \cap v \in Z \\ c4, u \notin Z \cup v \notin Z \end{cases} \\ Sineer &= \begin{cases} s1, u \in Z \cap v \in Z \\ s2, u \notin Z \cup v \notin Z \end{cases} \qquad Souter = \begin{cases} s3, u \in Z \cap v \in Z \\ s4, u \notin Z \cup v \notin Z \end{cases} \end{aligned} \tag{3.9}$$

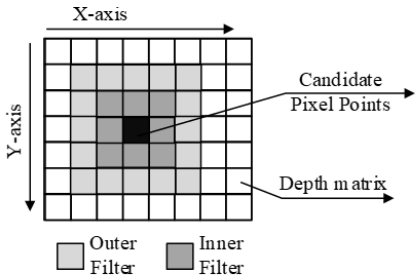

Fig. 3.3: Schematic diagram of filter principle

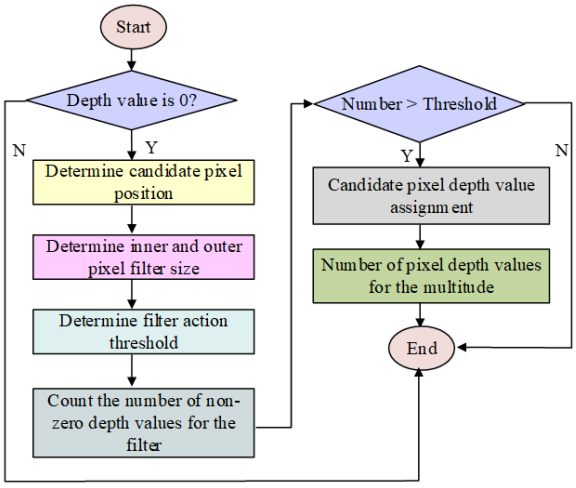

Fig. 3.4: Schematic diagram of the process of image restoration algorithm

In equation (3.9), Z represents the selected region range, $Nineer, Nouter$ represent the size of the inner and outer filters, and $Sineer, Souter$ represent the action threshold of the inner and outer filters. The flowchart of the image restoration algorithm is shown in Figure 2.4.

Variable parameter pixel filters can effectively reduce the number of information loss points and significantly improve the clarity of images. When Kinect sensors collect image information, there may also be random fluctuations in the depth values corresponding to the same pixel position. The study utilizes the weighted moving average algorithm to suppress random noise, and the algorithm process is shown in the figure. This algorithm assigns weights to the obtained depth frames and stores them in a queue data structure. It assigns larger values to depth frames that are closer in time, and the depth value weighting calculation method is shown in equation (3.10).

$$Snow = \frac{w1s1 + w2s2 + ...wnsn}{w1 + w2 + ...wn} \tag{3.10}$$

In equation (3.10), $Snow$ is the depth value matrix obtained by the sensor, $s1, s2, ..., sn$ is the depth value matrix of the previous depth frame, and $w1, w2, ..., wn$ is the weight value corresponding to the depth frame. At the same time, to improve the discrimination of image effects and reduce the subjectivity of contrast, Kinect sensors use classifiers to process depth information features and use these features to determine body parts.

The information features can be expressed as equation (3.11).

$$f\theta(I,x) = dI[x + \frac{u}{dI(x)}] - dI[x + \frac{v}{dI(x)}] \tag{3.11}$$

In equation (3.11), x is the value of the pixel position, dI is the depth value corresponding to the pixel value, $\frac{1}{dI(x)}$ is the offset normalization, and θ is the offset vector parameter.

3.3. Design of upper limb rehabilitation interaction based on multi-sensor fusion and interpersonal interaction. . The research designs the fusion of inertial sensors and Kinect sensors to achieve human motion trajectory tracking. Before data fusion, it is necessary to unify the coordinate systems of the two types of sensors. The study uses the geographic coordinate system as the intermediate coordinate system, and unifies the sensor coordinates into the intermediate coordinate system for coordinate conversion. The conversion method refers to the coordinate conversion method of inertial sensors. Subsequently, the sensor data is zero aligned, using the average output data of the two sensors as the data zero. Due to the different output frequencies of the two types of sensor data, the trajectory data calculated by the sensors is commented on and aligned before data fusion to ensure synchronization of data upload. The trajectory data for frequency alignment consists of the results of two inertial sensors and the Kinect sensor in the middle. Due to the small time interval, linear interpolation is used for data alignment to reduce system computational costs. The interpolated inertial sensor data at time $t2$ is expressed as equation (3.12).

$$x2 = x1\frac{t3 - t2}{t3 - t1} + x3\frac{t2 - t1}{t3 - t1} \tag{3.12}$$

In equation (3.12), $x1, x3$ represent the trajectory data of the inertial sensor at time $x1, x3$. Subsequently, considering that Kinect sensors are affected by occlusion during human motion trajectory tracking, resulting in data loss and jumps, it is necessary to process them. Research on the effectiveness judgment of sensor data based on confidence distance to improve the accuracy and stability of human upper limb motion trajectory tracking. The confidence distance measure can reflect the deviation between observed values, and its mathematical expression is shown in equation (3.13).

$$dij = 2\left|\int_{xi}^{xj} p(x\,|xi)dx\right| \tag{3.13}$$

In equation (3.13), xi, xj are the observed values of the trajectory data of the two sensors, and p is the trajectory data. The smaller the confidence distance measure, the closer the values are, and the calculated measure can form a confidence distance matrix. According to this matrix, a threshold conversion relationship is artificially set to verify the support between data, and the support value can be expressed as equation (3.14).

$$rij = \begin{cases} 0 & dij \geq \varepsilon 2 \\ 0.5 - 0.5(\frac{dij-\varepsilon}{\varepsilon 2-\varepsilon 1})^{0.5} & \varepsilon < dij < \varepsilon 2 \\ 0.5 & dij = \varepsilon \\ 0.5 + 0.5(\frac{\varepsilon-dij}{\varepsilon-\varepsilon 1})^{0.5} & \varepsilon 1 < dij < \varepsilon \\ 1 & dij \leq \varepsilon 1 \end{cases} \tag{3.14}$$

In equation (3.14), ε, $\varepsilon 1$, $\varepsilon 2$ represent the judgment threshold. The greater the support, the better the data compatibility between the two sensors. Subsequently, research was conducted on trajectory data fusion processing based on Bayesian estimation. Each dynamic verification process is a correction process of prior knowledge, and the conditional probability density function of the measured parameters can be expressed as equation (3.15).

$$p(\mu\,|x1, x2\,) = \frac{p(\mu, x1, x2)}{p(x1, x2)} \tag{3.15}$$

In equation (3.15), μ represents the measurement mean and follows a normal distribution, and $x1, x2$ represent the sensor trajectory data. The implementation of motion trajectory tracking in human-computer

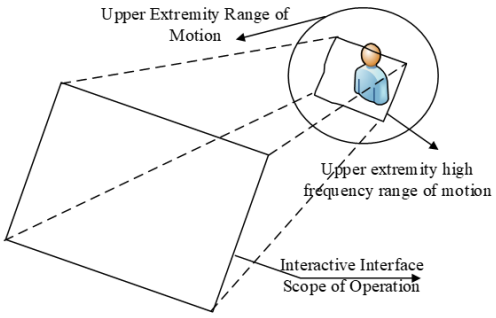

Fig. 3.5: Mapping relationship between upper limb movement range and interaction interface

interaction mainly relies on two interaction logics: "follow-up" and "instruction". The study analyzes the motion range of the Kinect sensor's two-dimensional plane in a "follow-up" interaction design, and maps the human motion range to the operating range of the interaction system, as shown in Figure 3.5.

After limiting the range of upper limb movement, the range of motion is approximately circular, and the study uses this range of motion for interactive mapping to expand the patient's motor ability. After setting the high-frequency range of upper limb movement, to ensure safety, it is necessary to reduce the proportion of this range by 10% as a safety margin, and any excess should also be treated according to the extreme value of the range boundary. When designing an interactive interface, calculate the aspect ratio of the interface and determine the maximum inscribed matrix within the high-frequency range of upper limb movement. The conversion coefficient can be expressed as equation (3.16).

$$\frac{u}{k} = \frac{v}{q'} = h \tag{3.16}$$

In equation (3.16), u, v represent the length and width of the inscribed rectangle, k, q' represent the length and width of the interactive interface, and h represents the conversion ratio coefficient. When using sensors for trajectory segmentation and feature matching, the "directive" interaction logic mainly relies on Kinect for Windows SDK2.0 tools for upper limb and hand state detection in human-machine interaction. Collect trajectory data by using hand stretching and curling as a sampling cycle, and then extract features from the trajectory information under time constraints, converting them into interactive interface instructions. The segmented trajectory data can obtain vector information and determine the direction of motion based on the starting point coordinates, and the azimuth of the vector coordinates can represent the vector orientation of the trajectory.

4. Training results analysis for upper limb rehabilitation robots. . The hardware part of the interaction system designed for research included a rehabilitation robot robotic arm, control cabinet, touch screen machine, display screen, inertial sensor, and Kinect sensor. The display screen was placed in front of the patient for data collection and rehabilitation exercise therapy. The study conducted tracking experiments using MATLAB attitude simulation tools and trajectory tracking experiments using the X-axis motion of an inertial sensor. The sensor accelerated and decelerated during the first and second half of its movement, and the obtained data was integrated to obtain its velocity and displacement change curves. The results are shown in Figure 3.1.

In Figure 4.1, there is a significant difference between the numerical values of the sensor data and the theoretical results after secondary integration processing, and during the sensor stop stage, the displacement data is still in a dynamic transformation state with time, and the error is constantly increasing. Subsequently, the tracking effect of the proposed error compensation algorithm was analyzed, and the results are shown in Figure 4.2.

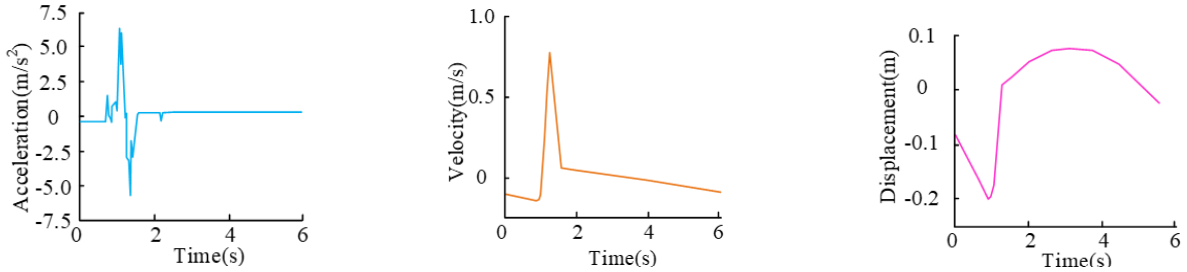

(a) Accelerometer Data

(b) Velocity under Acceleration frequency demen integration

(c) Displacement data under frequency domain integration of velocity

Fig. 4.1: Inertial sensor trajectory tracking results

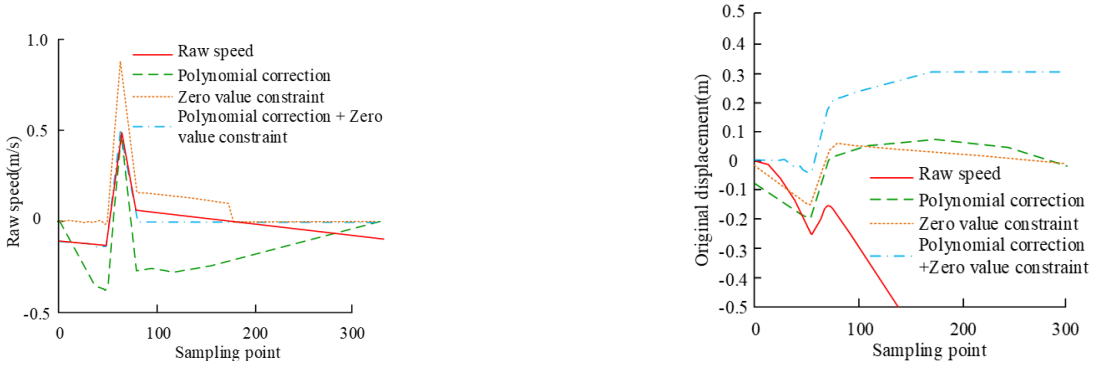

(a) Cumulative error removal results for velocity values

(b) Accumulated error removal results for displacement values

Fig. 4.2: Cumulative Error Removal Effect

In Figure 4.2, after the error correction of the sensor, its initial motion speed and displacement are not zero. Among them, polynomial-based correction algorithms were more prone to increasing cumulative errors due to the increase of time product in abnormal data analysis, and their improvement effect was not the best. The cumulative error results of sensors under zero value constraints and polynomial correction were significant, and the trajectory tracking accuracy was significantly improved. In terms of numerical values, the displacement of the sensor's X-axis remained stable at around 304.6mm, which was close to the theoretical value. The training time of different algorithms was analyzed, and the results are shown in Figure 4.3.

In Figure 4.3, the overall average time consumption of the algorithm proposed in the study is less than 1.5 seconds, and its curve gradually tends to stabilize when the sample points are greater than 100. Its performance was significantly better than other comparative algorithms. Subsequently, the proposed image restoration and noise reduction effect was analyzed, with filter sizes of 5 and 7, and corresponding threshold sizes of 3.1 and 3.2. The results are shown in Table 4.1.

In Table 4.1, the maximum fluctuation extremum and fluctuation variance of image denoising before processing reached 2.5 million and 10 or more, and its pixel loss was significant, with a mean square error value exceeding 22. The image loss situation was alleviated only by pixel filtering and weighted moving processing, but its depth fluctuation variance and image mean square error were both greater than the fusion algorithm

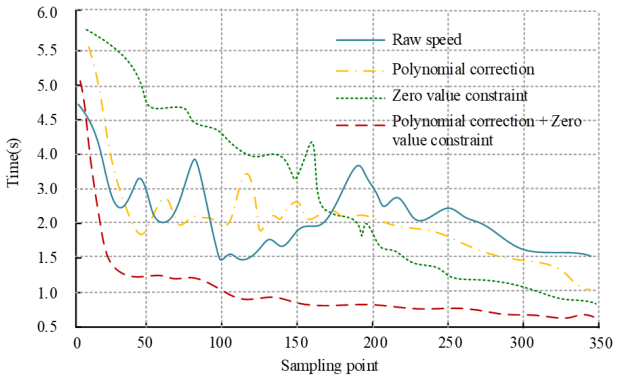

Fig. 4.3: Training time consumption situatione

Table 4.1: Evaluation Results of Image Restoration and Noise Reduction

Algorithms	Sum of fluctuating extremes(104)	Depth value fluctuation variance sum	Depth pixel loss points(104)	Image mean square error
Unused algorithms	255.17	12.45	3.19	22.67
Pixel Filter	188.41	8.59	1.55	3.06
Weighted Shift	173.98	9.36	2.58	13.70
Pixel filter + weighted shift	86.27	6.08	1.16	3.24

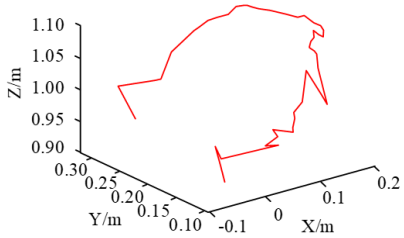

(a) Three-dimensional spatial trajectories of experimental movements

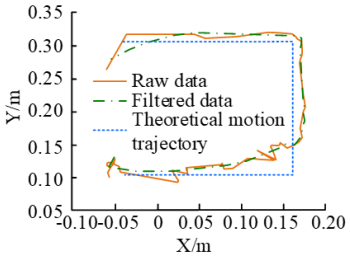

(b) Two-dimensional planar trajectory data

Fig. 4.4: Trajectory Data Results

proposed in the study. The image restoration effect of the proposed joint processing method was outstanding, with a loss value of 12000 pixels and a significant improvement in imaging quality. This study used the right hand as a reference to track the trajectory of upper limb movement, drove the arm with the right hand for rehabilitation spatial movement, and conducted experiments on the position coordinates of the wrist. The experimenter stood in front of the sensor and recorded motion tracking data. Figure 4.4 shows the trajectory results.

In Figure 4.4, the motion data of the original bone does not change steadily, with obvious fluctuations and some ”jumping” phenomenon in the data. After filtering the data, the processed three-dimensional spatial trajectory significantly improved its smoothness compared to the original data, with an error improvement of more than 20%. The instruction recognition results of the interactive system were analyzed and compared with traditional rehabilitation training methods. The results are shown in Figure 3.5.

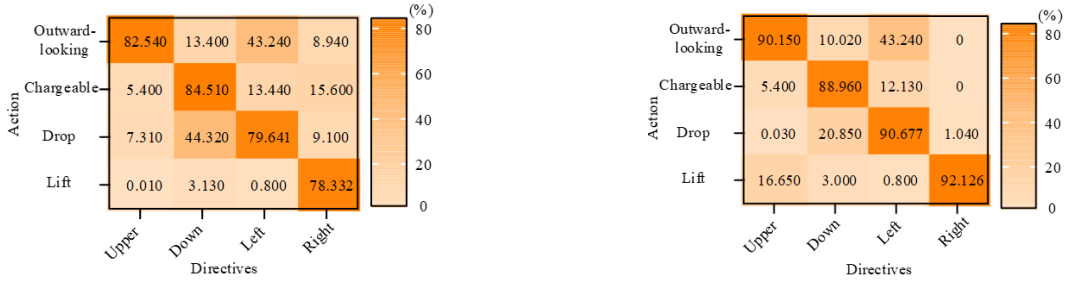

(a) Traditional Rehabilitation Interactive rehabilitation (b) Traditional Rehabilitation Interactive rehabilitation

Fig. 4.5: Instruction recognition results

Figure 4.5 shows the corresponding accuracy results of interaction instructions and robot actions. The results showed that the accuracy of interaction instructions and the four training actions of lifting, drooping, adduction, and abduction was 90.15%, 88.96%, 90.67%, and 92.12%, respectively, which were significantly higher than the traditional rehabilitation methods of 82.54%, 83.51%, 79.64%, and 78.33%. The rehabilitation actions of interactive training have good targeting and significant application effects.

5. Conclusion. This study analyzes an upper limb rehabilitation interaction system based on trajectory tracking and designs multiple sensors to track patient upper limb movement and trajectory data. The application results of the proposed interaction system in the study were analyzed, and the results showed that the error compensation algorithm can effectively improve the trajectory tracking accuracy. Compared with the cumulative error results of sensors under dual processing, the error was significantly reduced. The displacement of the sensor X-axis was stable at around 304.6mm, which was close to the theoretical value. The denoising processing of image data by sensors also effectively reduced information loss points (12000), and compared with the image fluctuation extreme value (>2.5 million) and fluctuation variance sum (>100000) before processing, the image quality improvement effect was significant. In the upper limb motion trajectory tracking results, the fluctuation of the filtered motion data was significantly reduced, and the error improvement was greater than 20%. Compared with traditional training methods, its accuracy in the four training actions of lifting, sagging, adduction, and abduction was 90.15%, 88.96%, 90.67%, and 92.12%, respectively, which was much higher than traditional rehabilitation results. Multi-sensor fusion and human-computer interaction can effectively improve the accuracy and stability of upper limb motion trajectory tracking. The proposed upper limb rehabilitation training system has improved the trajectory tracking of dry sensors and integrated multi-sensor data processing, which can effectively avoid the influence of accumulated errors on sensors, achieve higher accuracy in obtaining upper limb motion data, and achieve interaction with the rehabilitation training system. It has high stability and effectiveness. However, the shortcomings lie in the insufficient acquisition of dimensional information by sensors, and the scope of application verification scenarios still needs to be further expanded. In further research, it is necessary to consider and utilize data from different dimensions such as velocity and acceleration, and combine them with human upper limb kinematic models to provide more motion data for rehabilitation training. At the same time, machine learning technology can be used to automatically adjust the rehabilitation training plan based on the patient's rehabilitation progress and personal characteristics, provide remote rehabilitation support, and improve the convenience and accessibility of rehabilitation training. The proposed methods can be applied to more sensory games and virtual game designs, such as voice command control of the training process, or the use of VR technology to create immersive rehabilitation environments, to better improve the effectiveness and interactivity of rehabilitation training and treatment. Applying this method to healthcare and integrating it with other medical devices and health management systems, such as wearable health monitoring devices and electronic medical record systems, can achieve real-time monitoring of patient health status and provide more effective treatment plans for health management.

REFERENCES

[1] Vu, P., Chestek, C., Nason, S., Kung, T. & Cederna, P. The future of upper extremity rehabilitation robotics: research and practice. *Muscle & Nerve*. **61**, 708-718 (2020)

[2] Gupta, A., Singh, A., Verma, V., Mondal, A. & Gupta, M. Developments and clinical evaluations of robotic exoskeleton technology for human upper-limb rehabilitation. *Advanced Robotics*. **34**, 1023-1040 (2020)

[3] Xiao, W., Chen, K., Fan, J., Hou, Y., Kong, W. & AI-and, D. and assistive robotic system with intelligent PID controller based on RBF neural networks. *Neural Computing And Applications*. **35**, 16021-16035 (2023)

[4] Wang, Y., Wu, Q., Dey, N., Fong, S. & Ashour, A. Deep back propagation–long short-term memory network based upper-limb sEMG signal classification for automated rehabilitation. *Biocybernetics And Biomedical Engineering*. **40**, 987-1001 (2020)

[5] Sun, Q., Guo, S. & Zhang, L. Kinematic dexterity analysis of human-robot interaction of an upper limb rehabilitation robot. *Technology And Health Care*. **29**, 1029-1045 (2021)

[6] F. H. Yousuf, A. Alwarfali & F, H. Busedra. *Low-Cost Rehabilitation System For Upper Limb Amputees*. pp. 139-143 (2022)

[7] X. Chen, S. Zhang, K. Cao , C., W. Zhao & Yao.Development, J. of a Wearable Upper Limb Rehabilitation Robot Based on Reinforced Soft Pneumatic Actuators. *Hinese Journal Of Mechanical Engineering*. **35**, 1-9 (2022)

[8] Q. Wu & Chen.Development, Y. of an Intention-Based Adaptive Neural Cooperative Control Strategy for Upper-Limb Robotic Rehabilitation. *EEE Robotics And Automation Letters*. **6**, 335-342 (2021)

[9] Li, X., Yang, Q. & Song, R. Performance-based hybrid control of a cable-driven upper-limb rehabilitation robot. *IEEE Transactions On Biomedical Engineering*. **68**, 1351-1359 (2020)

[10] Meng, Q., Jiao, Z., Yu, H. & Zhang, W. Design and evaluation of a novel upper limb rehabilitation robot with space training based on an end effector. *Mechanical Sciences*. **12**, 639-648 (2021)

[11] Zhang, J., Zeng, H., Li, X., Xu, G., Li, Y. & Song, A. Bayesian optimization for assist-as-needed controller in robot-assisted upper limb training based on energy information. *Robotica*. **41**, 3101-3115 (2023)

[12] Wang, J., Li, Y. & An., A. Dynamic parameter identification of upper-limb rehabilitation robot system based on variable parameter particle swarm optimisation. *IET Cyber-Systems And Robotics*. **2**, 140-148 (2020)

[13] Mirrashid, N. ŮŤE Alibeiki, SM Rakhtala. *Development And Control Of An Upper Limb Rehabilitation Robot Via Ant Colony Optimization-PID And Fuzzy-PID Controllers*. **35**, 1488-1493 (2022)

[14] Wu, Q. & Chen, Y. Development of an intention-based adaptive neural cooperative control strategy for upper-limb robotic rehabilitation. *IEEE Robotics And Automation Letters*. **6**, 335-342 (2020)

[15] Meng, Q., Yue, Y., Li, S. & Yu., H. Electromyogram-based motion compensation control for the upper limb rehabilitation robot in active training. *Mechanical Sciences*. **13**, 675-685 (2022)

[16] Rossa, C., Najafi, M., Tavakoli, M. & Adams, K. Robotic rehabilitation and assistance for individuals with movement disorders based on a kinematic model of the upper limb. *IEEE Transactions On Medical Robotics And Bionics*. **3**, 190-203 (2021)

[17] Zhou, J., Li, Z., Li, X., Wang, X. & Song, R. Human–robot cooperation control based on trajectory deformation algorithm for a lower limb rehabilitation robot. *IEEE/ASME Transactions On Mechatronics*. **26**, 3128-3138 (2021)

[18] Li., L. Mirror motion recognition method about upper limb rehabilitation robot based on sEMG. *Journal Of Computational Methods In Sciences And Engineering*. **21**, 1021-1029 (2021)

[19] Cai, S., Li, G., Su, E., Wei, X., Huang, S., Ma, K., Zheng, H. & Xie, L. Real-time detection of compensatory patterns in patients with stroke to reduce compensation during robotic rehabilitation therapy. *IEEE Journal Of Biomedical And Health Informatics*. **24**, 2630-2638 (2020)

[20] Proietti, T., O'Neill, C., Hohimer, C., Nuckols, K., Clarke, M., Zhou, Y., Lin, D. & Walsh, C. Sensing and control of a multi-joint soft wearable robot for upper-limb assistance and rehabilitation. *IEEE Robotics And Automation Letters*. **6**, 2381-2388 (2021)

[21] M. Assad-Uz-Zaman, M. R. Islam, M. H. Rahman, Y. C. Wang & Mcgonigle.Kinect, E. Controlled NAO Robot for Telerehabilitation. *Ournal Of Intelligent Systems*. **30**, 224-239 (2020)

[22] N. Z. Azlan & Journal, N. . (2021)

[23] Z. Tongtong, Z. Yue, Design, C. & Simulation, K. of a Novel 7-DOF Upper Limb Rehabilitation Exoskeleton Robot. *Ournal Of Mechanical Transmission*. **46**, 66-72 (2022)

[24] H. Yan, H. Wang, P. Chen, J. Niu & Wang.Configuration, X. Design of an Upper Limb Rehabilitation Robot with a Generalized Shoulder Joint. *Pplied Sciences*. **11** pp. 5 (2021)

[25] Nicholson-Smith, C., Mehrabi, V., Atashzar, S. & Patel, R. A multi-functional lower-and upper-limb stroke rehabilitation robot. *IEEE Transactions On Medical Robotics And Bionics*. **2**, 549-552 (2020)

[26] Gupta, A., Singh, A., Verma, V., Mondal, A. & Gupta, M. Developments and clinical evaluations of robotic exoskeleton technology for human upper-limb rehabilitation. *Advanced Robotics*. **34**, 1023-1040 (2020)

[27] Lee, S., Adans-Dester, C., O'Brien, A., Vergara-Diaz, G., Black-Schaffer, R. & Zafonte, R. Predicting and monitoring upper-limb rehabilitation outcomes using clinical and wearable sensor data in brain injury survivors. *IEEE Transactions On Biomedical Engineering*. **68**, 1871-1881 (2020)

Edited by: Bradha Madhavan
Special issue on: High-performance Computing Algorithms for Material Sciences
Received: Feb 3, 2024
Accepted: Jul 4, 2024